Crystal-chemistry of sulfates from the Apuan Alps (Tuscany, Italy). VIII. New data on khademite, $Al(SO_4)F(H_2O)_5$

DANIELA MAURO[1*], CRISTIAN BIAGIONI[1], MARCO PASERO[1], and FEDERICA ZACCARINI[2]

[1]*Dipartimento di Scienze della Terra, Università di Pisa, Via Santa Maria 53, 56126 Pisa, Italy*
[2]*Department of Applied Geological Sciences and Geophysics, University of Leoben, Peter Tunner Str. 5, A-8700 Leoben, Austria*

e-mail address: daniela.mauro@dst.unipi.it*

Mineralogical Society

This is a 'preproof' accepted article for Mineralogical Magazine. This version may be subject to change during the production process.
DOI: 10.1180/mgm.2020.51

ABSTRACT

Khademite, ideally $Al(SO_4)F(H_2O)_5$, from the Monte Arsiccio mine (Apuan Alps, Tuscany, Italy) has been characterized through quantitative electron microprobe analysis, micro-Raman spectroscopy, and single-crystal X-ray diffraction. Khademite occurs as colorless to whitish tabular crystals, up to 5 mm across, or as sugary aggregates formed by colorless and shiny individuals less than 0.5 mm in size. Electron microprobe analysis (in wt% - average of twenty spot analyses) gave: SO_3 35.43, Al_2O_3 21.27, F 6.92, H_2O_{calc} 39.73, sum 103.35, –O = F 2.92, total 100.43. On the basis of 10 anions per formula unit, assuming the occurrence of 5 H_2O groups and 1 (F+OH) atom per formula unit, its chemical formula can be written as $Al_{0.96}S_{1.02}O_4(F_{0.84}OH_{0.16})_{\Sigma 1.00}\cdot 5H_2O$. The Raman spectrum of khademite is characterized by the occurrence of vibrational modes of SO_4 groups and by broad and strong bands due to the O–H stretching modes. Khademite is orthorhombic, space group *Pcab*, with unit-cell parameters a = 11.1713(2), b = 13.0432(3), c = 10.8815(2) Å, V = 1585.54(5) $Å^3$, Z = 8. The crystal structure refinement converged to R_1 = 0.0293 on the basis of 2359 unique reflections with $F_o > 4\sigma(F_o)$ and 152 refined parameters. The crystal structure of khademite is characterized by the alternation, along **b**, of two distinct kinds of {010} layers, one formed by [001] rows of isolated Al-centered octahedra, connected to each other through H-bonds, and the other showing isolated SO_4 groups. Along **b**, oxygen atoms belonging to SO_4 groups act as acceptor of H-bonds from H_2O groups coordinating Al atoms. The new data improved the description of the H-bonds in khademite and led us to discuss about the possible existence of its OH-analogue, rostite. In addition, Raman spectroscopic data were collected on the same crystal used for the crystal-chemical characterization, allowing a comparison with previous results.

Keywords: khademite, fluorine, fluo-sulfate, crystal structure, hydrogen bonds, Raman spectroscopy, Monte Arsiccio mine, Apuan Alps.

Introduction

Sulfate minerals play a central role in governing the release and transport of acidity and potential environmentally critical elements following pyrite oxidation (*e.g.*, Jerz and Rimstidt, 2003; Hammarstrom *et al.*, 2003, 2005). Recently, the finding of high thallium contents in pyrite ore deposits from the southern Apuan Alps (northern Tuscany, Italy; D'Orazio *et al.*, 2017) promoted the characterization of secondary mineral assemblages allowing the collection of mineralogical and geochemical data.

The presence of sulfate assemblages related to the weathering of pyrite ores has been known since the second half of the 19th Century (*e.g.*, D'Achiardi, 1872). However, only in the last decade modern mineralogical data have been collected, with the identification of well-crystallized sulfates in the Fornovolasco and Monte Arsiccio mines. In the former locality, the new mineral species volaschioite, $Fe_4(SO_4)O_2(OH)_6 \cdot 2H_2O$, as well as Tl-bearing varieties of alum-(K) and voltaite, were found (Biagioni *et al.*, 2011, 2020). Moreover, Monte Arsiccio proved to be an extraordinary laboratory for the study of sulfate minerals, providing the mineral systematics with three new K-Fe sulfates (giacovazzoite, scordariite, and magnanelliite – Biagioni *et al.*, 2019a; 2019b; 2019c), and several other species, among which world-class specimens of coquimbite (Mauro *et al.*, 2020).

A peculiar feature of the Fornovolasco and Monte Arsiccio sulfate assemblages is represented by the rare occurrence of fluo-sulfates. Mauro *et al.* (2019) described wilcoxite from the Fornovolasco mine, reporting new crystal structure data and improving the knowledge of its H-bond system. Recently, another fluo-sulfate, khademite, was identified at the Monte Arsiccio mine. The current definition of khademite is the result of a long and debated history summarized by Košek *et al.* (2019). As a matter of fact, a modern and full characterization of khademite is still lacking, since Bachet *et al.* (1981) did not give any chemical analysis and no further crystal structure refinements were reported. The finding at the Monte Arsiccio mine permitted the collection of a new set of good-quality data, integrating electron microprobe, spectroscopic, and single-crystal X-ray diffraction analyses, along with a thoughful discussion of previous available data.

Experimental

Studied specimen

Khademite from the Monte Arsiccio mine occurs as colorless to whitish tabular crystals, up to 5 mm across (Fig. 1), associated with krausite, halotrichite, and coquimbite. These samples were carefully investigated during the present study.

Chemical analysis

Quantitative chemical data were collected on the same tabular crystal used for single-crystal X-ray diffraction study using a Superprobe JEOL JXA 8200 electron microprobe at the Eugen F. Stumpfl laboratory, Leoben University, Austria. The analytical conditions were: WDS mode, accelerating voltage 15 kV, beam current 10 nA, beam diameter 20 μm. Standards (element, emission line) were: pyrite (S*K*α), kaersutite (Al*K*α), and fluorite (F*K*α). Iron was sought but was found below the detection limit. ZAF routine was applied for the

correction of recorded raw data. Counting times were 20 s for peak and 10 s for left and right background, respectively. Quantitative chemical data are given in Table 1.

Micro-Raman spectroscopy

Micro-Raman spectra of khademite were collected on the same polished sample used for the quantitative chemical analysis using a Horiba Jobin-Yvon XploRA Plus apparatus, with a 50× objective lens and the 532 nm line of a solid-state laser attenuated to 25% (*i.e.*, 6.25 mW). The spectra were collected in the range between 100 to 4000 cm^{-1}, through multiple acquisitions (3) with single counting times of 60 s. Backscattered radiation was analyzed with a 1200 gr/mm grating monochromator. Figure 2 shows the collected Raman spectrum, whereas Table 2 gives the observed Raman bands and their interpretation. Band fitting of the O–H stretching region was performed using *Fityk* (Wojdyr, 2010).

X-ray crystallography

X-ray intensity data were collected using a Bruker Smart Breeze diffractometer (50 kV, 30 mA) equipped with a Photon II CCD detector. Graphite-monochromatized Mo*K*α radiation was used. The detector-to-crystal working distance was 50 mm. Intensity data were integrated and corrected for Lorentz-polarization, background effects, and absorption, using the package of software *Apex*3 (Bruker AXS Inc., 2016), resulting in a set of 17,350 reflections. The refined unit-cell parameters are a = 11.1713(2), b = 13.0432(3), c = 10.8815(2) Å, V = 1585.54(5) $Å^3$, Z = 8. Space group *Pcab* was suggested by the statistical tests on $|E|$ values ($|E^2-1|$ = 0.953) and by the examination of systematic absences. The crystal structure of khademite was refined using *Shelxl*-2018 (Sheldrick, 2015), starting from the atomic coordinates given by Bachet *et al.* (1981). Taking into account the results of the electron microprobe analysis, the site scattering at the Al, S, F, O, and H sites was modeled using neutral site scattering curves taken from the *International Tables for Crystallography* (Wilson, 1992). Although the coordinates of H atoms were given by Bachet *et al.* (1981), their positions for the sample from Monte Arsiccio have been sought in the difference-Fourier maps. Soft restraints were applied to O–H bonds, in order to avoid too short distances. The crystal structure refinement of khademite, after several cycles of anisotropic refinement (with the exception of H atoms, which were refined isotropically), converged to R_1 = 0.0293 for 2359 unique reflections with $F_o > 4\sigma(F_o)$ and 152 refined parameters. Details of data collection and refinement are given in Table 3. Fractional atomic coordinates and isotropic or equivalent isotropic displacement parameters are reported in Table 4, whereas selected bond distances are shown in Table 5. Finally, the geometrical features of the hydrogen bonds are given in Table 6. Table 7 reports the bond-valence sum (BVS) calculations, performed using the bond parameters of Brese and O'Keeffe (1991) for Al–O, Al–F, and S–O bonds; simplified bond-valences, agreeing with Brown and Altermatt (1981), are reported for H-bonds.

Results and discussions

Chemical data

The occurrence of fluorine in the crystal structure of khademite has been debated for a long time. Indeed, the detection and quantification of this light element is not an easy task

(*e.g.*, Stormer *et al.*, 1993; Raudsepp, 1995; Ottolini *et al.*, 2000). Quantitative chemical data of khademite, including F, have been reported by Žáček and Povondra (1988), Williams and Cesbron (1983), and Košek *et al.* (2019).

Data given in Table 1, recalculated on the basis of 10 anions per formula unit (pfu), assuming the occurrence of 5 H_2O and 1 (F+OH) pfu, in agreement with our structural data, allow to write the following chemical formula for khademite from the Monte Arsiccio mine: $Al_{0.96}S_{1.02}O_4(F_{0.84}OH_{0.16})_{\Sigma 1.00}\cdot 5H_2O$. It agrees with the ideal formula $Al(SO_4)F\cdot 5H_2O$. The studied sample was chemically homogeneous and no significant F variations were observed among the twenty spot analyses, suggesting rather constant F/OH ratios.

Micro-Raman spectroscopy

The Raman spectrum of khademite (Fig. 2) is characterized by the occurrence of the four fundamental modes of the SO_4 group and by the O–H stretching vibration modes due to the H_2O groups hosted in its crystal structure. Two spectral regions can be recognized, *i.e.*, between 100-1200 cm^{-1} and between 2500-3800 cm^{-1}. The former region (Fig. 2a) is characterized by bending and stretching modes of the SO_4 group, located between 400 and 1130 cm^{-1}, and by the vibration modes of Al–φ (φ = O, F) bonds and/or to lattice vibration modes, below 400 cm^{-1}. The symmetric bending modes (ν_2) of the SO_4 group are characterized by bands at 417, 432, 499, and 523 cm^{-1} whereas the bands due to the antisymmetric bending modes (ν_4) occur at 566, 587, 616, and 632 cm^{-1}. The strongest band at 993 cm^{-1} is due to the symmetrical stretching mode (ν_1) of the SO_4 group. The weaker bands at 1079 and 1128 cm^{-1} are attributed to the antisymmetrical stretching mode (ν_3) of the SO_4 group. In the region between 3000 and 4000 cm^{-1} a broad multi-component band related to the O–H stretching modes of H_2O groups occur. This band can be compared with that observed by Košek *et al.* (2019) who established the peak position through a basic peak-finding routine, reporting the presence of three bands at 3040, 3177, and 3404 cm^{-1}; these values agree with those measured (using a similar peak-finding routine) in the sample of khademite from Monte Arsiccio, i.e., 3053, 3183, and 3406 cm^{-1}. In addition, a shoulder at 2967 cm^{-1} was observed. In addition, a fitting of the spectrum using theoretical peak shapes (*i.e.*, Voigt function) was performed from the sample from Monte Arsiccio, revealing the occurrence of at least four main bands, at 2966, 3047, 3197, and 3420 cm^{-1} (Fig. 2b). These components are likely related to the occurrence of relatively strong H-bonds in khademite, as shown in Table 6 and discussed below. For instance, six out of the ten O⋯O distances reported in Table 6 range between 2.662 and 2.692 Å, corresponding to frequencies of 3053 and 3166 cm^{-1} according to the relationship of Libowitzky (1999). The maxima of the broad Raman bands are in agreement with such an interpretation. Košek *et al.* (2019) interpreted the Raman band at 3404 cm^{-1} as due to the hydroxyl stretching mode. However, this is not proved by structural data and disagrees with previous data reported for sulfate minerals. Indeed, the occurrence of the O–H stretching modes due to the hydroxyl group should be observed at higher wavenumber (*e.g.*, Kong *et al.*, 2011; Ventruti *et al.*, 2016). In addition, three bands at 3524, 3521, and 3584 cm^{-1} were observed for not-symmetry related OH units occurring in the crystal structure of creedite, $Ca_3Al_2(SO_4)(OH)_2F_8\cdot 2H_2O$, by Frost *et al.*, (2013a). Finally, as it will be discussed below, the possible occurrence of an OH-group in khademite may be related

to a relatively long O···O distances, giving rise to a band at wavenumbers higher than 3500 cm^{-1}.

Bending modes due to the H–O–H bonds were observed at 1606 cm^{-1}. On the contrary, Košek *et al.* (2019) did not observe any bending modes in their Czech sample, whereas Frost et al. (2015) reported two bending modes at 1605 and 1692 cm^{-1} in rostite. Table 2 compares our results with available micro-Raman spectroscopic data collected on both khademite and its OH-analogue rostite. Data for the Monte Arsiccio sample are in good agreement, within experimental uncertainties, with those given by Frost *et al.* (2015) and Košek *et al.* (2019). On the contrary, the sample of khademite studied by Frost *et al*. (2013b) shows a fully different Raman spectrum; this disagreement is likely due to the fact that these authors studied a not fully-characterized specimen. It is very likely that their spectrum does not belong to khademite.

Single-crystal X-ray diffraction

Description of the crystal structure: cation coordinations and general features

Three cation sites, namely Al(1), Al(2), and S, and ten anion positions occur in the crystal structure of khademite, along with ten H sites.

Aluminum is hosted at the Al(1) and Al(2) sites. Both positions show an octahedral coordination; in the former site, Al atoms are coordinated by H_2O groups only, whereas in the Al(2) site, four H_2O groups and two F anions are bonded to Al. Bond distances at the Al(1) polyhedra range between 1.85 and 1.89 Å, in agreement with those previously reported by Bachet *et al.* (1981), *i.e.*, 1.85 and 1.89 Å. The Al(2)-centered polyhedron is more distorted than the Al(1)-centered polyhedron with bond distances ranging from 1.73 and 1.95 Å. According to Bachet *et al.* (1981), the shortest distance can be attributed to the Al–F bond. The longest distance is the Al(2)–Ow(3). It is worth noting that this distance is longer than all the other Al–Ow distances observed in the crystal structure of khademite and it is related to the fact that the H_2O group at Ow(3) is the only H_2O group receveing an H-bond; in fact, the elongation of the Al–Ow distance favour a reduction of the BVS and the possibility to accept the additional H-bond from Ow(6) (Table 7). The average <Al–O> distances are 1.878 and 1.858 Å for Al(1) and Al(2) sites, respectively. The BVS for the Al(1) and Al(2) site (Table 7) are 3.26 and 3.14 valence units (v.u), respectively. The isolated SO_4 group has an average <S–O> distance of 1.472 Å, in agreement with those reported in sulfate minerals by Hawthorne *et al*. (2000), *i.e*., 1.473 Å. The corresponding BVS at the S site is 6.03 v.u (Table 7).

The crystal structure of khademite (Fig. 3) can be described as a layered structure. Indeed, it is characterized by the alternation of two different kinds of {010} layers. The first one (hereafter indicated as A) is formed by two independent isolated Al-centered octahedra, having chemical composition $Al(H_2O)_6$ and $Al(H_2O)_4F_2$, respectively. These octahedra are connected through H-bonds, forming rows running along [001]. Every A layer has chemical composition $[Al_4(H_2O)_{20}F_4]^{8+}$. The other layer (B layer) is formed only by isolated SO_4 groups; in each layer, four independent SO_4 groups occur. The connection between adjacent A and B layers occurs through the oxygen atoms of SO_4 groups that act as acceptor of H-bonds from H_2O coordinating Al atoms. In each unit cell, two A and B layers occur. Consequently, the unit-cell content is $2 \times [Al_4(H_2O)_{20}F_4]^{8+} + 2 \times [(SO_4)_4]^{8-} =$

$Al_8(SO_4)_8F_8(H_2O)_{40}$ (Z = 1), corresponding to the end-member formula of khademite, $Al(SO_4)F(H_2O)_5$ (Z = 8).

Hydrogen bonding

Table 7 highlights that all the atoms hosted at the ten independent anion positions occurring in the crystal structure of khademite are underbonded. Two groups of anions can be distinguished; a first group has BVS of ~ 1.5 v.u, whereas a second group has BVS ranging between 0.4 and 0.6 v.u. This observation suggests that H-bonds play a key role in the stabilization of the crystal structure of khademite. The geometrical features of H-bonds given in Table 6 match those found by Bachet *et al*. (1981). On the basis of the O···O distances *d*, the ten H-bonds can be grouped into three types: (1) very strong [d = 2.52 Å – one H-bond], (2) strong [2.6 < d < 2.7 Å – eight H-bonds], and (3) weak [d ~ 2.9 Å – one H-bond]. All O atoms bonded to S have BVS ~ 1.5 v.u. and each of these O atoms receives two similar strong H-bonds. The valence sum rule therefore suggests each of these bonds be 0.25 v.u. in strength; this values is in agreement with Figure 2 of Brown and Altermatt (1985) as well as the relationship of Ferraris and Ivaldi (1988), giving BVS for these strong H-bonds ranging between 0.23 and 0.27 v.u. Consequently, in Table 7 all strong H-bonds can be assigned a bond strength of 0.25 v.u. On similar ground, the very strong H-bond can be assigned a value of 0.30 v.u., considering that the acceptor is F (see Figure 1 in Brown and Altermatt, 1985), whereas 0.15 v.u. are attributed to the weak H-bond.

In details, the H_2O groups coordinating the Al(1) and Al(2) sites, namely Ow(2)-Ow(5) act as donor in strong H-bonds to the O atoms belonging to the SO_4 group. The Ow(6) is donor of a strong H-bond to an oxygen atom belonging to the SO_4 group, i.e., O(2), and of a weak bond to Ow(3), as discussed above. The F atom is acceptor of a very strong H-bond from Ow(5). The role of F as acceptor of H-bonds agrees with the previous structural model proposed by Bachet *et al*. (1981) and was observed in other rare sulfate minerals [*e.g*., wilcoxite, $MgAl(SO_4)_2F{\cdot}17H_2O$; Mauro *et al*., 2019].

Can rostite be a valid mineral species?

Khademite and its (OH)-analogue rostite have a troubled history, as summarized by Košek *et al*. (2019). These authors stated that the crystal structure study of khademite performed by Bachet *et al*. (1981) "*found that the atomic positions in the structure were so small that they require the presence of fluorine, and that the presence of OH in the structure was not possible.*" It is not clear what Košek *et al*. (2019) mean when they state that "*the atomic positions* […] *were so small*". A critical reading of the original paper by Bachet *et al*. (1981) reveals the actual reason leading the authors to hypothesize the occurrence of F, without the support of any chemical data. Indeed, Bachet *et al*. (1981) were not able to locate the H atom related to the OH group and they observed a slight electron density residual on that O atom, supporting the occurrence of a slightly heavier atom. In this hypothesis, Bachet *et al*. (1981) were supported by the association of khademite with another fluo-sulfate, wilcoxite. Finally, the examination of the H-bond system around F suggested the impossibility to locate an OH group at this position.

The impossibility to locate an OH group in the crystal structure of khademite could have some implications for the actual existence of its OH-analogue, rostite, ideally

$Al(SO_4)(OH)(H_2O)_5$. Indeed, to the best of our knowledge, only a sample of rostite from the Cetine di Cotorniano mine (Tuscany, Italy) has been reported in literature, with OH slightly dominant over F (Sabelli, 1984). However, in agreement with Košek *et al*. (2019), the correctness of the-chemical data of Sabelli (1984) is questionable.

Bachet *et al*. (1981) described the coordination environment of F atoms, highlighting that they are acceptor of H-bonds from Ow(5). If F is replaced by OH, then OH would be donor to Ow(2), with a bond distance of ~3.19 Å but with a too small Ow(5)–OH–Ow(2) angle of ~ 55°. For this reason, Bachet *et al*. (1981) wrote that it was impossible to replace F with OH groups in khademite. Taking into account the result of the refinement performed on the sample from Monte Arsiccio, the structural features described by Bachet *et al*. (1981) are confirmed (Fig. 4a). As regards the possible existence of the OH-analogue, we argue that the replacement of F by OH might favour an increase in the Al–φ distance, e.g., up to 1.84 Å, in order to supply a similar BVS (0.60 v.u.). The strong contribution from H(52) could be retained; taking into account a similar H···O distance as observed in khademite, a bond strength of ~ 0.35 v.u. can be proposed on the basis of Brown and Altermatt (1985). In order to have a BVS of ~ 2 v.u. at the O atom occurring at the OH position, a strong donor contribution (e.g., ~ 0.95 v.u) is required. This would necessitate a distant O acting as acceptor, that would receive a weak H-bond (e.g., ~ 0.05 v.u.). In the crystal structure of khademite there are two possible O anions, Ow(2) (as proposed by Bachet *et al*., 1981) and O(4). Whereas Ow(2) was excluded by Bachet *et al*. (1981) in order to avoid too small Ow(5)–OH–Ow(2) angle (i.e., ~ 55°), a reasonable angle of ~ 95° can be formed with O(4). Figure 4b shows a hypothetical H-bond scheme involving these atoms. The BVS at O(4) would be 2.06 v.u.; if one consider the distance measured in the crystal structure of khademite (~3.25 Å), a bond strength of 0.10 v.u. can be calculated using the relationship of Ferraris and Ivaldi (1988), whereas a value close to 0 v.u. can be hypothesized following Brown and Altermatt (1985). Minor structural changes could likely be associated with the F-OH replacement, improving the structural fitting with respect to this chemical substitution.

This discussion does not aim to prove that rostite actually exist. Indeed, as written above, the only available data are those of Sabelli (1984) and they are questionable. On the contrary, we aim at demonstrating that there are no apparent impediment to the occupation of univalent anion site by OH within the khademite structure, in disagreement with the hypothesis of Bachet *et al*. (1981). Rostite may be a valid mineral species, but more sound chemical data are required to confirm its existence.

Conclusions

The occurrence of khademite at the Monte Arsiccio mine allowed the collection of high-quality single-crystal X-ray diffraction data and electron microprobe analyses, improving the crystal-chemical knowledge of this rare fluo-sulfate and confirming previous results reported by Bachet *et al*. (1981). Taking into account that all H_2O groups are bonded to Al atoms, the chemical formula of khademite could be written as $Al(SO_4)F(H_2O)_5$.

In addition, the critical examination of available Raman spectroscopic data highlighted some discrepancies in the published spectra. Indeed, whereas the data reported by Frost *et al*. (2015) for rostite from Le Cetine di Cotorniano (Italy) and Košek *et al.* (2019) for khademite

from Libušín (Czech Republic) agree, within experimental uncertainties, with those collected on the Monte Arsiccio sample, the Raman spectrum of khademite reported by Frost *et al*. (2013b) does not fit with previous and current results. These observations have a two-fold implication. On the one hand, the strong similarity between the Raman spectra of rostite and khademite confirms the uncertain distinction between these two phases, although current structural data do not show any impediment to the existence of the OH-analogue of khademite. On the other hand, the discrepancy observed between the spectra of khademite and the data published by Frost *et al*. (2013b) highlights the importance of using crystal-chemically well-characterized samples during Raman studies.

Acknowledgements

Mario Bianchini is thanked for providing us with the specimen of khademite from the Monte Arsiccio mine. CB acknowledges financial support from the University of Pisa through the project P.R.A. 2018-2019 "Georisorse e Ambiente" (Grant No. PRA_2018_41). The authors are grateful to the University Centrum for Applied Geosciences (UCAG) for the access to the E. F. Stumpfl electron microprobe laboratory. The authors wish to thank Mark Cooper for his critical revision, that greatly improved the discussion of the H-bonds in khademite and suggested a comparison with rostite. The comments of other two anonymous reviewers were also appreciated.

References

Bachet, B., Cesbron, F. and Chevalier, R. (1981) Structure cristalline de la khadémite $Al(SO_4)F{\cdot}5H_2O$. *Bulletin de Minéralogie*, **104**, 19–22.

Biagioni, C., Bonaccorsi E., Orlandi P. (2011) Volaschioite, $Fe^{3+}{}_4(SO_4)O_2(OH)_6{\cdot}2H_2O$, a new mineral species from Fornovolasco, Apuan Alps, Tuscany, Italy. *Canadian Mineralogist*, **49**, 605–614.

Biagioni, C., Bindi, L., Mauro, D. and Pasero, M. (2019a) Crystal chemistry of sulfates from the Apuan Alps (Tuscany, Italy). IV. Giacovazzoite, $K_5Fe^{3+}{}_3O(SO_4)_6(H_2O)_9{\cdot}H_2O$, the natural analogue of the β-Maus's Salt and its dehydration product. *Physics and Chemistry of Minerals*, **47**, 7.

Biagioni, C., Bindi, L., Mauro, D. and Hålenius, U. (2019b) Crystal chemistry of sulfates from the Apuan Alps (Tuscany, Italy). V. Scordariite, $K_8(Fe^{3+}{}_{0.67}\square_{0.33})[Fe^{3+}{}_3O(SO_4)_6(H_2O)_3]_2(H_2O)_{11}$: a new metavoltine-related mineral. *Minerals*, **9**, 702.

Biagioni, C., Bindi, L. and Kampf, A.R. (2019c) Crystal-chemistry of sulfates from the Apuan Alps (Tuscany, Italy). VII. Magnanelliite, $K_3Fe^{3+}{}_2(SO_4)_4\ (OH)(H_2O)_2$, a new sulfate from the Monte Arsiccio mine. *Minerals*, **9**, 779.

Biagioni, C., Mauro, D., Pasero, M., Bonaccorsi, E., Lepore, G.O., Zaccarini, F. and Skogby H. (2020) Crystal-chemistry of sulfates from the Apuan Alps (Tuscany, Italy). VI. Tl-bearing alum-(K) and voltaite from the Fornovolasco mining complex. *American Mineralogist*, doi.org/10.2138/am-2020-7320.

Brese, N.E. and O'Keeffe, M. (1991) Bond-valence parameters for solids. *Acta Crystallographica*, **B47**, 192–197.

Brown, I.D. and Altermatt, D. (1985) Bond-valence parameters obtained from a systematic analysis of the Inorganic Crystal Structure Database. Acta Crystallographica, **B41**, 244–247.

Bruker, AXS Inc. (2016) APEX 3. Bruker Advanced X-ray Solutions, Madison, Wisconsin, USA.

D'Achiardi, A. (1872). Mineralogia della Toscana. Volume 1. Tipografia Nistri, Pisa, 278 p.

D'Orazio, M., Biagioni, C., Dini, A., and Vezzoni, S. (2017) Thallium-rich pyrite ores from the Apuan Alps, Tuscany, Italy: constraints for their origin and environmental concerns. *Mineralium Deposita*, **52**, 687–707.

Ferraris, G. and Ivaldi, G. (1988) Bond valence vs bond length in O···O hydrogen bonds. *Acta Crystallographica*, **B44**, 341–344.

Frost, R.L., Xi, Y. Scholz, R., Lòpez, A. and Granja, A. (2013a) Infrared and Raman spectroscopic characterisation of the sulphate mineral creedite – $Ca_3Al_2SO_4(F,OH){\cdot}2H_2O$ – and in comparison with the alums. *Spectrochimica Acta Part A: Molecular and Biomolecular Spectroscopy*, **109**, 201–205.

Frost, R.L., Scholz, R., Lòpez, A. and Xi, Y. (2013b) Vibrational spectroscopic characterization of the sulphate mineral khademite $Al(SO_4)F{\cdot}5(H_2O)$. *Spectrochimica Acta Part A: Molecular and Biomolecular Spectroscopy*, **116**, 165–169.

Frost, R.L., Scholz, R., Lima, R.M. and Lòpez, A. (2015) SEM, EDS and vibrational spectroscopic study of the sulphate mineral rostite $AlSO_4(OH,F){\cdot}5(H_2O)$. *Spectrochimica Acta Part A: Molecular and Biomolecular Spectroscopy*, **151**, 616–620.

Hammarstrom, J.M., Seal II, R.R., Meier, A.L. and Jackson, J.C. (2003) Weathering of sulfidic shale and copper mine waste: secondary minerals and metal cycling in Great Smoky Mountains National Park, Tennessee, and North Carolina, USA. *Environmental Geology*, **45**, 35–57.

Hammarstrom, J.M., Seal II, R.R., Meier, A.L. and Kornfeld, J.M. (2005) Secondary sulfate minerals associated with acid drainage in the eastern US: recycling of metals and acidity in surficial environments. *Chemical Geology*, **215**, 407–431.

Hawthorne, F.C., Krivovichev, S.V. and Burns, P.C. (2000) The crystal chemistry of sulfate minerals. In: Sulfate minerals-crystallography, geochemistry and environmental significance. *Review in Mineralogy and Geochemistry*, **40**, 1–101.

Jerz, J.K. and Rimstidt, J.D. (2003) Efflorescent iron sulfate minerals: Paragenesis, relative stability, and environmental impact. *American Mineralogist*, **88**, 1919–1932.

Kong, W.G., Wang, A., Freeman, J.J. and Sobron, P. (2011) A comprehensive spectroscopic study of synthetic Fe^{2+}, Fe^{3+}, Mg^{2+}, and Al^{3+} copiapite by Raman, XRD, LIBS, MIR, and vis-NIR. *Journal of Raman Spectroscopy*, **42**, 1120–1129.

Košek, F., Žáček, V., Škoda, R., Laufek, F., Jehlička, J. (2019) New mineralogical data for khademite (orthorhombic $AlSO_4F{\cdot}5H_2O$) and the story of rostite (orthorhombic $AlSO_4F{\cdot}5H_2O$) from Libušín, near Kladno, Czech Republic. *Journal of Molecular Structure*, **1175**, 208–213.

Libowitzky, E. (1999) Correlation of O–H stretching frequencies and O–H···O hydrogen bond lengths in minerals. *Monatshefte für Chemie*, **130**, 1047–1059.

Mauro, D., Biagioni, C., Pasero, M. and Skogby, H. (2019) Crystal-chemistry of sulfates from Apuan Alps (Tuscany, Italy). III. Mg-rich sulfate assemblages from the Fornovolasco mining complex. *Atti della Società Toscana di Scienze Naturali, Memorie*, **126**, 34–44.

Mauro, D., Biagioni, C., Pasero, M. Skogby, H. and Zaccarini, F. (2020) Redefinition of coquimbite, $AlFe^{3+}_3(SO_4)_6(H_2O)_{12}{\cdot}6H_2O$. *Mineralogical Magazine*, **84**, 275–282.

Ottolini, L., Cámara, F. and Bigi, S. (2000) An investigation of matrix effects in the analysis of fluorine in humite-group minerals by EMPA, SIMS, and SREF. *American Mineralogist*, **85**, 89–102.

Raudsepp, M. (1995) Recent advances in the electron-probe micro-analysis of minerals for the light elements. *Canadian Mineralogist*, **33**, 203–218.

Sabelli C. (1984) I minerali delle Cetine di Cotorniano (SI): I solfati dimorfi jurbanite e rostite. *Periodico di Mineralogia*, **53**, 53–65.

Sheldrick, G.M. (2015) Crystal Structure Refinement with SHELXL. *Acta Crystallographica*, **C71**, 3–8.

Stormer, Jr., J.C, Pierson, M.L. and Tacker, R.C. (1993) Variation of F and Cl X-ray intensity due to anisotropic diffusion in apatite during electron microprobe analysis. *American Mineralogist*, **78**, 641–648.

Ventruti, G., Della Ventura, G., Bellatreccia, F., Lacalamita, M., and Schingaro, E. (2016) Hydrogen bond system and vibrational spectroscopy of the sulfate fibroferrite, $Fe(OH)SO_4{\cdot}5H_2O$. *European Journal of Mineralogy*, **28**, 943–952.

Williams, S.A. and Cesbron, F.P. (1983) Wilcoxite and lannonite, two new fluosulphates from Catron County, New Mexico. *Mineralogical Magazine*, **47**, 37–40.

Wilson, A.J.C. (1992) International Tables for Crystallography. Volume C. Kluwer, Dordrecht.

Wojdyr, M. (2010) Fityk: a general-purpose peak fitting program. *Journal of Applied Crystallography*, **43**, 1126–1128.

Žáček, V. and Povondra, P. (1988) New mineralogical data for rostite from Lisbušín, Central Bohemia, Czechoslovakia. *Neues Jahrbuch für Mineralogie, Monatshefte,* **10**, 476–480.

Table captions

Table 1. Electron microprobe data of khademite.
Table 2. Raman bands (cm^{-1}) of khademite and their assignments.
Table 3. Summary of crystal data and parameters describing data collection and refinement for khademite.
Table 4. Sites, fractional atom coordinates and isotropic (*) or equivalent isotropic displacement parameters in khademite.
Table 5. Selected bond distances (Å) in khademite.
Table 6. Hydrogen-bond lengths (in Å) and angles (in °) for khademite.
Table 7. Bond-valence sums (in valence unit) for khademite.

Figure captions

Fig. 1. Colorless tabular crystals of khademite, up to 5 mm in size, associated with halotrichite. Monte Arsiccio mine, Apuan Alps, Italy.
Fig. 2. Raman spectrum of khademite and band positions in the regions 100-1200 cm^{-1} (a) and 2500-3800 cm^{-1} (b); in (b) the cumulative curve is shown in green whereas fitted bands are red. The plot of residuals and the R^2 value are also shown.
Fig. 3. The crystal structure of khademite (a), as seen down **a**; letters A and B indicate the two different {010} layers. Dashed and dotted blue lines represent F···O distances and H···O distances shorter than 1.95 Å, respectively. Unit cell is shown as dashed black lines. Polyhedra: light blue = Al(1)-centered octahedra; violet = Al(2)-centered octahedra (c); yellow = S-centered tetrahedra; Circles: red = O atoms of the SO_4 group; light blue = O atoms of the H_2O groups; pink = H atoms; light green = F atoms. Details of the coordination of Al(1) and Al(2) are shown in (b) and (c), respectively; bond distances (in Å) are shown.
Fig. 4. The H-bond system around F atom in khademite (a) and an hypothetical configuration with F replaced by OH (b). Same symbols as in Figure 3. Bond strengths around the monovalent anion are shown in italics (in v.u.).

Table 1. Electron microprobe data of khademite.

Oxide	wt% (n = 20)	range	σ
SO_3	35.43	34.05-36.41	0.69
Al_2O_3	21.27	20.40-22.01	0.44
F	6.92	6.54-7.16	0.20
H_2O_{calc}*	39.73		
Sum	103.35		
–O = F	-2.92		
Total	100.43		

*Calculated in agreement with structural data. σ = estimated standard deviation.

Table 2. Raman bands (cm^{-1}) of khademite and their assignments.

This study	Frost *et al.* (2013b)	Frost *et al.* (2015)	Košek *et al*. (2019)	Assignments
127 vw, 150 w, 300 w, 337 w	113 vw, 150 vw, 192 vw,226 vw, 253 vw, 324 vw	169 vw, 203 vw 216 vw, 281 vw, 295 vw, 307 vw, 319 vw, 340vw	130 w, 150 vw, 168 vw, 216 vw, 294 vw, 306 vw, 342 vw	Al–O and lattice modes
420 w, 432 vw, 499 w, 523 vw	455 w, 505 vw, 534 vw	420 w, 434 vw, 504 m, 530 vw	420 w, 433 vw, 504 m, 528vw	$\nu_2 (SO_4)$
566 w, 587 m, 616 m, 632 w	618 w	570 w, 590 m, 620 w, 632w	569 w, 589 m, 619 w, 632w	$\nu_4 (SO_4)$
993 vs	975 m, 991 vs	991 vs	990 vs	$\nu_1 (SO_4)$
1079 m, 1128 w	1104 vw, 1132 w	1070w, 1083 m, 1131 w, 1145vw	1081 m, 1131 m	$\nu_3 (SO_4)$
1606 w	1609 vw	1605 w, 1692 w	-	$\nu_2 (H_2O)$
2967, 3053, 3183, 3406	2991, 3146, 3380	2764, 2948 3082, 3155, 3322, 3295	3040, 3177 3404	ν_1 and ν_3 (H_2O)

Table 3. Summary of crystal data and parameters describing data collection and refinement for khademite.

Crystal data	
Structural formula	$AlSO_4F(H_2O)_5$
Crystal size (mm^3)	0.18 × 0.15 × 0.13
Cell setting, space group	Orthorhombic, *Pcab*
a(Å)	11.1713(2)
b(Å)	13.0432(3)
c(Å)	10.8815(2)
V ($Å^3$)	1585.54(5)
Z	8
Data collection and refinement	
Radiation, wavelength (Å)	Mo*K*α, λ = 0.71073
Temperature (K)	293
Maximum observed 2θ (°)	63.04
Measured reflections	17350
Unique reflections	2600
Reflections $F_o > 4\sigma(F_o)$	2359
R_{int} after absorption correction	0.0196
Rσ	0.0133
Range of *h*, *k*, *l*	$-16 \le h \le 16$, $-19 \le k \le 16$, $-13 \le l \le 15$
R [F_o>4 σ F_o]	0.0293
R (all data)	0.0332
wR (on F_o^2)	0.0858
Goof	1.138
Number of least-squares parameters	152
Maximum and minum residual peak (*e*/$Å^3$)	0.32 [at 0.71 Å from O(2)] -0.49 (at 0.36 Å from S)

Table 4. Sites, fractional atom coordinates and isotropic (*) or equivalent isotropic displacement parameters in khademite.

Site	*x*/*a*	*y*/*b*	*z*/*c*	U_{eq} (Å^2)
Al(1)	0	½	½	0.01120(11)
Al(2)	0	½	0	0.01252(11)
S	0.23846(3)	0.24741(2)	0.24697(2)	0.01431(9)
O(1)	0.16892(9)	0.25489(6)	0.13246(8)	0.02521(19)
O(2)	0.30519(10)	0.14999(8)	0.24632(7)	0.0313(2)
O(3)	0.15860(9)	0.25014(6)	0.35448(8)	0.0247(2)
O(4)	0.32053(9)	0.33547(8)	0.25373(7)	0.0288(2)
F	0.02937(7)	0.50938(5)	0.15592(6)	0.02092(15)
Ow(2)	0.01006(7)	0.37567(6)	0.58852(7)	0.01751(16)
Ow(3)	0.14302(7)	0.41497(6)	-0.02101(7)	0.01918(16)
Ow(4)	-0.09380(8)	0.38237(6)	0.02869(8)	0.02325(18)
Ow(5)	0.06920(8)	0.43591(6)	0.36595(7)	0.01916(17)
Ow(6)	-0.15403(7)	0.46351(7)	0.44224(7)	0.01960(17)
H(21)	-0.0520(15)	0.3324(14)	0.6011(17)	0.042(5)*
H(22)	0.0662(16)	0.3610(17)	0.6476(16)	0.050(6)*
H(31)	0.1498(17)	0.3608(13)	0.0315(16)	0.042(5)*
H(32)	0.148(2)	0.3879(16)	-0.0974(15)	0.054(6)*
H(41)	-0.1181(16)	0.3395(12)	-0.0305(14)	0.036(5)*
H(42)	-0.1231(19)	0.3699(16)	0.0968(19)	0.049(6)*
H(51)	0.0907(19)	0.3690(13)	0.3631(19)	0.057(6)*
H(52)	0.0576(18)	0.4617(16)	0.2911(14)	0.045(5)*
H(61)	-0.2242(17)	0.4922(15)	0.468(2)	0.060(7)*
H(62)	-0.161(2)	0.4245(15)	0.3723(15)	0.055(6)*

Table 5. Selected bond distances (Å) in khademite.

Al(1)	– Ow(5)	1.8505(7) ×2
	– Ow(2)	1.8894(7) ×2
	– Ow(6)	1.8927(8) ×2
	<Al(1) – O>	1.878
Al(2)	– F	1.7324(6) ×2
	– Ow(4)	1.8841(8) ×2
	– Ow(3)	1.9584(8) ×2
	<Al(2) – O>	1.858
S	– O(4)	1.4714(9)
	– O(1)	1.4716(9)
	– O(3)	1.4717(8)
	– O(2)	1.4732(9)
	<S – O>	1.472

Table 6. Hydrogen-bond lengths (Å) and angles (°) for khademite.

Donor (*D*)	*D*–H	Acceptor (*A*)	H···*A*	*D*–H···*A* Angle	*D*···*A*
Ow(2)–H(21)	0.905(15)	O(1)	1.765(15)	176.9(18)	2.6696(12)
Ow(2)–H(22)	0.918(15)	O(4)	1.745(15)	177(2)	2.6624(11)
Ow(3)–H(31)	0.912(14)	O(1)	1.778(14)	177.8(19)	2.6892(11)
Ow(3)–H(32)	0.905(15)	O(4)	1.793(15)	172(2)	2.6925(11)
Ow(4)–H(41)	0.895(14)	O(3)	1.771(14)	176.5(18)	2.6654(11)
Ow(4)–H(42)	0.83(2)	O(2)	1.83(2)	176(2)	2.6669(12)
Ow(5)–H(51)	0.906(16)	O(3)	1.728(16)	169(2)	2.6237(11)
Ow(5)–H(52)	0.891(15)	F	1.627(15)	175(2)	2.518(10)
Ow(6)–H(61)	0.912(16)	Ow(3)	2.000(16)	167(19)	2.8961(12)
Ow(6)–H(62)	0.919(15)	O(2)	1.722(15)	172(2)	2.6351(11)

Table 7. Bond-valence sums (in valence unit) for khademite.

	Al(1)	Al(2)	S	Σanion	H(21)	H(22)	H(31)	H(32)	H(41)	H(42)	H(51)	H(52)	H(61)	H(62)	Σanions*
O(1)			1.51	1.51	0.25		0.25								2.01
O(2)			1.50	1.50						0.25				0.25	2.00
O(3)			1.51	1.51					0.25		0.25				2.01
O(4)			1.51	1.51		0.25		0.25							2.01
F		$0.60^{\downarrow\times2}$		0.60								0.30			0.90
OW(2)	$0.53^{\downarrow\times2}$			0.53	0.75	0.75									2.03
OW(3)		$0.44^{\downarrow\times2}$		0.44			0.75	0.75					0.15		2.09
OW(4)		$0.53^{\downarrow\times2}$		0.53					0.75	0.75					2.03
OW(5)	$0.58^{\downarrow\times2}$			0.58							0.75	0.70			1.93
OW(6)	$0.52^{\downarrow\times2}$			0.52									0.85	0.75	2.12
Σcations	3.26	3.14	6.03		1.00	1.00	1.00	1.00	1.00	1.00	1.00	1.00	1.00	1.00	

Note: right superscripts indicate the number of equivalent bonds involving anions. The bond-valence sums at H sites have been simplified. The symbol * indicates the BVS at anion sites after correction for H-bonds.

This is a 'preproof' accepted article for Mineralogical Magazine. This version may be subject to change during the production process.
DOI: 10.1180/mgm.2020.51

Fig. 1. Colorless tabular crystals of khademite, up to 5 mm in size, associated with halotrichite. Monte Arsiccio mine, Apuan Alps, Italy.

Mineralogical Society

This is a 'preproof' accepted article for Mineralogical Magazine. This version may be subject to change during the production process.
DOI: 10.1180/mgm.2020.51

Fig. 2. Raman spectrum of khademite and band positions in the regions 100-1200 cm^{-1} (a) and 2500-3800 cm^{-1} (b); in (b) the cumulative curve is shown in green whereas fitted bands are red. The plot of residuals and the R^2 value are also shown.

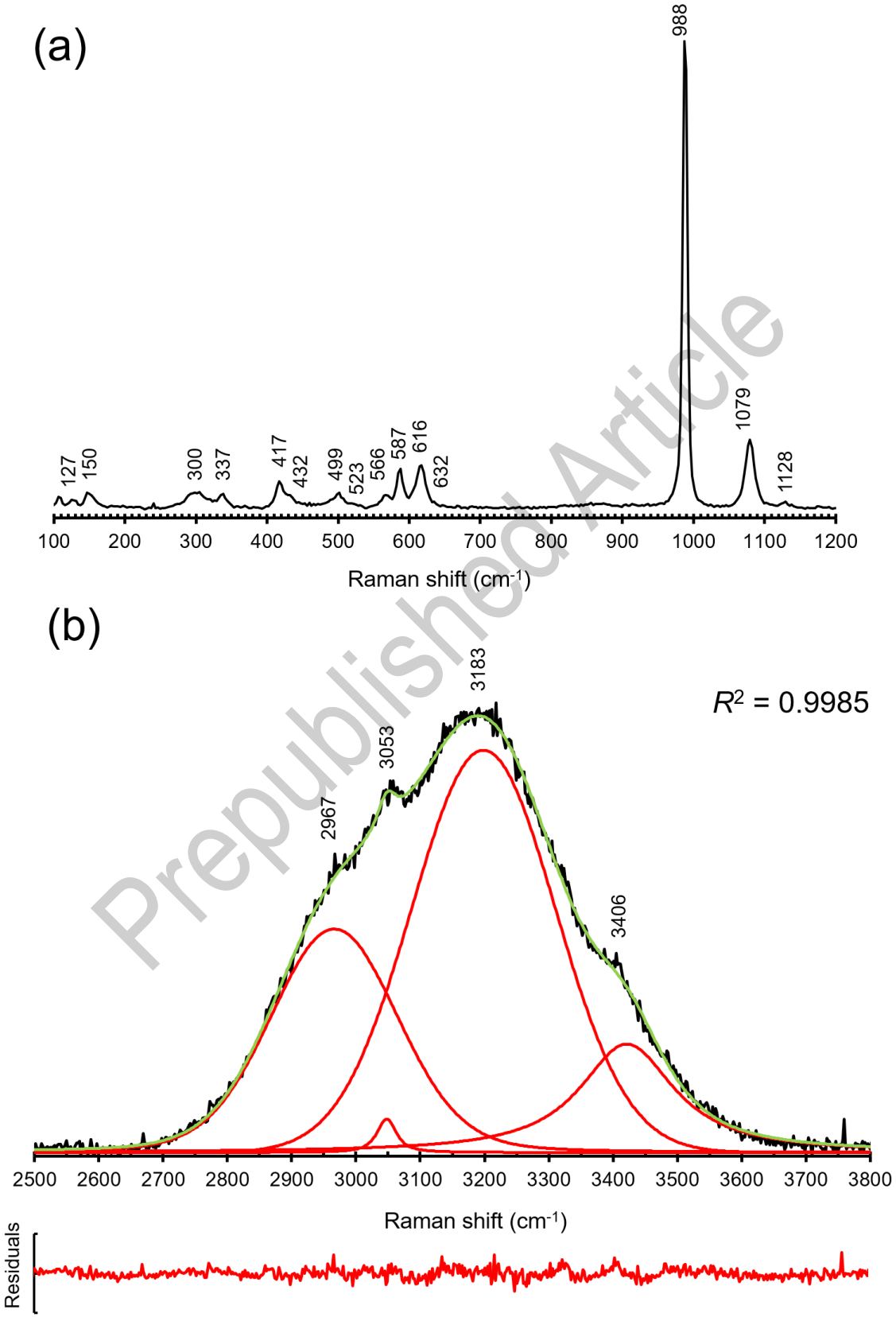

Fig. 3. The crystal structure of khademite (a), as seen down **a**; letters A and B indicate the two different {010} layers. Dashed and dotted blue lines represent F···O distances and H···O distances shorter than 1.95 Å, respectively. Unit cell is shown as dashed black lines. Polyhedra: light blue = Al(1)-centered octahedra; violet = Al(2)-centered octahedra (c); yellow = S-centered tetrahedra; Circles: red = O atoms of the SO_4 group; light blue = O atoms of the H_2O groups; pink = H atoms; light green = F atoms. Details of the coordination of Al(1) and Al(2) are shown in (b) and (c), respectively; bond distances (in Å) are shown.

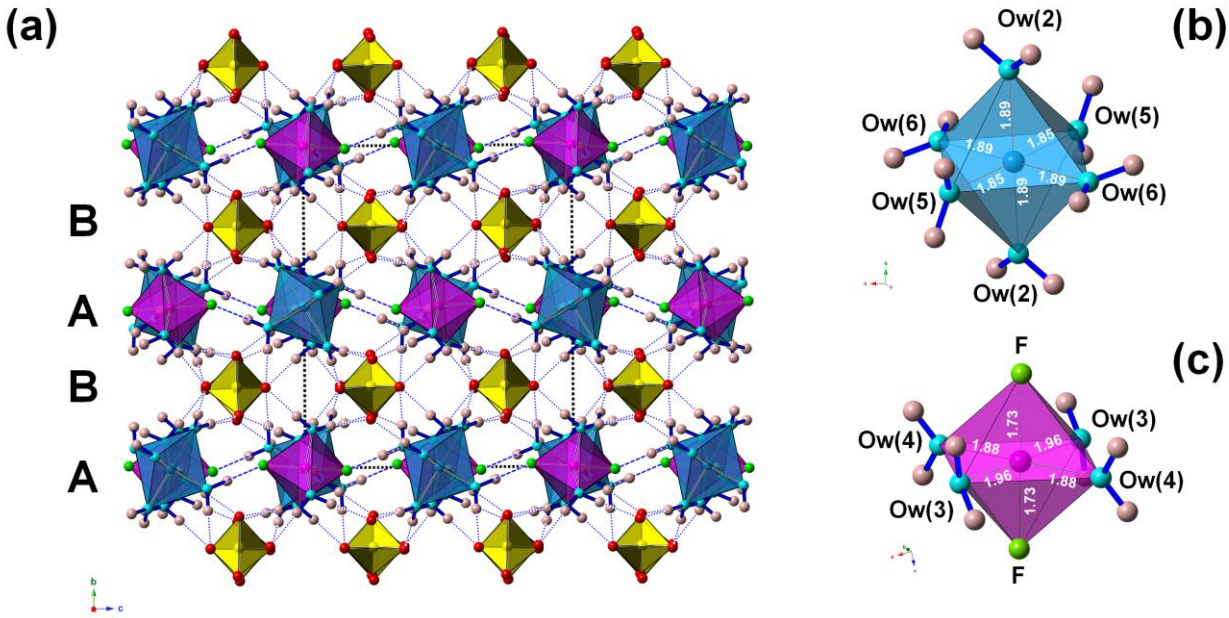

Fig. 4. The H-bond system around F atom in khademite (a) and an hypothetical configuration with F replaced by OH (b). Same symbols as in Figure 3. Bond strengths around the monovalent anion are shown in italics (in v.u.).